Optimal control of wave-packet isotope separation

M. Leibscher and I. Sh. Averbukh
Department of Chemical Physics, The Weizmann Institute of Science, Rehovot 76100, Israel
(Received 6 August 2000; published 13 March 2001)

We present an optimal control approach to the process of molecular isotope separation by exciting vibrational wave packets with femtosecond laser pulses. In the weak-field limit, we developed an optimization procedure for designing shaped laser pulses leading to the best selectivity in the two-photon ionization processes. Several control scenarios are identified, which mainly belong to two groups. The first takes advantage of the revival phenomenon, which allows one to find times at which excited wave packets of different isotopes are well localized and spatially separated in the intramolecular space. The second is based on isotopically selective quantum interference between several wave packets excited in the same molecular potential by a designed sequence of laser pulses. Simulations have been done for the isotopic mixture of $^{79}Br_2$ and $^{81}Br_2$ molecules, which was used in the first experiments on wave-packet isotope separation.

DOI: 10.1103/PhysRevA.63.043407 PACS number(s): 32.80.Qk, 32.10.Bi

I. INTRODUCTION

New developments in the technology of producing femtosecond laser pulses have expanded the possibilities of investigating and controlling intramolecular processes [1,2]. The ability to shape laser pulses [3] has made it possible to optimize their phase and amplitude to create specially tailored quantum wave packets and to manipulate their dynamics (see, e.g., [4]). It has been predicted in the past that reaction selectivity can be controlled by varying the relative phase and amplitudes of several light fields [5] or by pulse shaping [6], and the general field of quantum optimal control [7,8] has provided a number of tools to treat the problem. Recently, the ability to control photoinduced chemical reactions has been demonstrated experimentally for photodissociation reaction of iron pentacarbonyl [9]. Another goal of quantum molecular control is to steer intramolecular dynamics. Considerable work has been done in controlling wave-packet dynamics with specially designed laser fields for various purposes such as optimizing wave-packet squeezing [10] or wave-packet recurrences [11].

Femtosecond wave-packet techniques have also been used to investigate isotope selective molecular dynamics [12,13]. Recently, an isotope separation method was introduced that is based on the preparation of spatially localized vibrational wave packets [14]. Traditional laser isotope separation techniques [15] rely on small isotopic shifts of energy levels [16]. They require extremely narrowband tunable light sources as well as detailed knowledge of the spectroscopy of the system to achieve isotopically selective excitation. In contrast, wave-packet isotope separation [14] makes use of the differences in the free evolution of the wave packets in different isotopes. In this scheme, a short laser pulse excites virtually identical vibrational wave packets in an excited molecular potential. Initially, the wave packets undergo periodic oscillatory motion. If they behaved exactly like classical particles, the small isotopic mass difference would eventually lead to spatial separation of the wave packets. This separation is most pronounced when the classical motion of two isotopically different wave packets becomes 180° out of phase. However, quantum-mechanical spreading due to the anharmonicity of molecular potentials leads to a spatial overlap of the wave packets, thus preventing their separation. Since the delocalization time is, in general, much smaller than the time needed for separation, the above quasiclassical separation scenario fails. A solution to this problem comes from the phenomena of revivals and fractional revivals [17–28] of wave packets. As the vibrational wave packets consist of a finite number of discrete states, they show strong localization (revivals) at a number of specific instants of time after the initial spreading. If, in addition, the classical oscillations of the isotopically different wave packets are out of phase with each other during one of these revival events, such a situation favors the process of isotope separation. For instance, an additional laser pulse may be applied to the system that ionizes only one isotopic component of the mixture. This is possible, because the photonic energy needed for ionization depends strongly on the position of the wave packet in the electronic potential.

These heuristic arguments demonstrated their effectiveness in the experiment [14] in which a considerable separation ratio was achieved without any additional attempt to optimize the separation process. The motivation of the present study is twofold. First of all, we want to apply the powerful technique of quantum optimal control [7] to this problem to review the potential and limitations of the method when more sophisticated field manipulations (pulse shaping) are allowed. Next, we hope that the automatic nature of the optimal control algorithms will allow us to reveal other scenarios of wave-packet isotope separation in addition to that found in [14] on a more intuitive basis. Both objectives were successfully fulfilled, as described in the following sections.

In Sec. II, we present a description of a linear optimization procedure for separation of an isotopic mixture of diatomic molecules. In Sec. III, we apply the method to a mixture containing $^{79}Br_2$ and $^{81}Br_2$ molecules. We discuss various mechanisms that lead to isotope separation and describe how they depend on such parameters as the interaction time between molecules and laser field and on the spectral range of the excitation field.

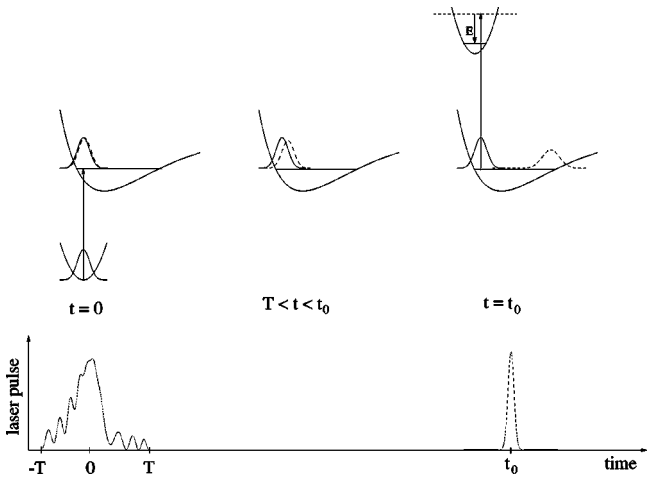

FIG. 1. Principle of wave-packet isotope separation: During the time interval $-T<t<T$, a laser pulse excites vibrational wave packets of an isotopic mixture of diatomic molecules. Between $t=T$ and $t=t_0$, the wave packets evolve freely in the excited potential $|e\rangle$ until a short pulse at $t=t_0$ ionizes a part of the molecules.

II. LINEAR OPTIMIZATION PROCEDURE

The model we use to optimize the wave-packet isotope separation is sketched in Fig. 1. We consider a mixture of diatomic molecules containing two different isotopes. The molecules interact with a laser field during the time interval $-T<t<T$. The laser field excites vibrational wave packets in the upper molecular potential. After the interaction, the wave packets evolve freely in this potential until a second, short laser pulse ionizes a part of the molecules at time $t=t_0$. With the help of the linear optimal control approach, we will be able to find those fields that result in the maximal difference of the ionization probability of different isotopes. The ionized species enriched in a certain isotopic component can then be extracted by standard electromagnetic means.

To discriminate against trivial, isotopically selective monochromatic solutions, we restrict the interaction time by $\tau_{\rm int}=2T$ (T is a free parameter) and focus on separation mechanisms based on dynamic effects.

We assume that the molecules are initially in their lowest vibrational state $|0\rangle$ of the ground electronic potential $|g\rangle$. The first laser pulse excites a set of molecular vibrational states $|n\rangle$ of the upper electronic potential $|e\rangle$. The vibrational wave function in this potential can be expanded as ($\hbar=1$)

$$|\psi^{[i]}(t)\rangle=\sum_n c_n^{[i]}(t)\exp[-iE_n^{[i]}t]|n\rangle, \tag{1}$$

where index i denotes the isotope. Here, we neglect the excitation of continuum states that do not contribute to the second step of our separation process. The electronic potentials and the vibrational eigenfunctions are approximately the same for both isotopes, and the isotopic mass difference is reflected in the vibrational energies $E_n^{[i]}$. Assuming that the laser field is weak, and using the Franck-Condon approximation, one obtains the following expression for the coefficients $c_n^{[i]}(t)$ in first-order perturbation theory:

$$c_n^{[i]}(T)=i\mu_{ge}\langle n|0\rangle\int_{-T}^{T}dt'\mathcal{E}(t')\exp[i\omega_{n,0}^{[i]}t'], \tag{2}$$

where $\mu_{ge}\equiv\langle g|\hat{\mu}|e\rangle$ is the transition dipole moment between the ground and excited electronic states, $\mathcal{E}(t)$ is the shape of the laser pulse, and $\omega_{n,0}^{[i]}\equiv(E_n^{[i]}-E_0^{[i]})$. At $t=t_0$, a second laser pulse ionizes the prepared wave packet. In the dipole approximation, the coupling between the excited potential $|e\rangle$ and the energy continuum $|E'\rangle$ in the ionic potential $|i\rangle$ is [29]

$$W(t)=-\int_0^\infty dE'\mu_{ei}(E')\mathcal{E}_{\rm ion}(t)|i,E'\rangle\langle e|, \tag{3}$$

where $\mathcal{E}_{\rm ion}(t)$ is the shape of the ionizing pulse. The electronic eigenstates of the ionic Hamiltonian are denoted by $|i,E'\rangle$. They describe free electrons with the kinetic energy $E'=k'^2/(2m_e)$ as well as the core electrons. In general, the transition dipole moment between the intermediate electronic state and the ionic state, $\mu_{ei}(E')$, depends on E'. Hence the E' dependence is generally weak [30]; we set for simplicity $\mu_{ei}(E')=\mu_{ei}$ in the relevant energy interval [29]. The probability of finding the ionized molecule in the vibrational state $|f\rangle$ and the free electron having kinetic energy E' is then [31]

$$P_{f,E'}^{[i]}=|\mu_{ei}|^2|\sum_n\langle f|n\rangle c_n^{[i]}(T)G(E'+E_f^{[i]}-E_n^{[i]})|^2,$$

where

$$G(E'+E_f^{[i]}-E_n^{[i]})=\int dt'\mathcal{E}_{\rm ion}(t')\times\exp[-i(E'+E_f^{[i]}-E_n^{[i]})t']. \tag{4}$$

For short ionization pulses, we may assume that $E_f^{[1]}\approx E_f^{[2]}\equiv E_f$. To obtain the total ionic signal, that is, the total probability to ionize the molecules, we sum over all vibrational states of the ionic potential and integrate over the electronic continuum,

$$P^{[i]}(t_0)=\sum_f\int dE'P_{f,E'}^{[i]}(t_0). \tag{5}$$

In our linear control scheme, we try to optimize the shape of the first pumping field only, while considering the second pulse as a ''short'' one. That means that the molecules stay ''frozen'' during the ionization process. For this, the bandwidth of the ionization pulse should be bigger than the energy widths of the wave packet in the excited potential. At the same time, this pulse may be relatively long compared to the period of high-frequency oscillations in the ionic potential, so that only a single (ground) vibrational ionic state contributes to the sum Eq. (5). In this limit, the ionization

probability is proportional to the spatial overlap between the wave packet $|\psi^{[i]}(t_0)\rangle$ and the ground vibrational state in the ionic potential

$$P^{[i]}(t_0)=|\mu_{ei}|^2\mathcal{E}_0^2|\langle f=0|\psi^{[i]}(t_0)\rangle|^2. \tag{6}$$

In Eq. (6), the ion signal is a functional of the first pumping pulse, while the only important parameter depending on the second (ionizing) pulse is the time of its arrival, t_0. Generally, the ionized molecules are more compressed compared to the neutral ones, and hence the equilibrium position of the ionic potential is shifted towards a smaller internuclear distance. Therefore, the ionic signal is large when the wave packet $|\psi^{[i]}(t_0)\rangle$ is localized near the left turning point, small when the wave packet is in the right half of the potential, and it takes intermediate values when the wave packet is spread over the whole potential.

A measure for the efficiency of separation is the difference in the ionic signals of different isotopes at fixed energy of the laser pulse. Our objective is to design, for a given interaction time $\tau_{\rm int}$, a laser pulse $\mathcal{E}(t)$ that maximizes the difference $P^{[2]}-P^{[1]}$ of the ionic signals. The functional we want to optimize is, therefore,

$$J=P^{[1]}(t_0,T)-P^{[2]}(t_0,T)-\lambda I, \tag{7}$$

where $P^{[i]}(t_0,T)$ are the ionic signals, Eq. (6), and I is the total energy of the pumping field,

$$I=\int_{-T}^{T}dt|\mathcal{E}(t)|^2. \tag{8}$$

The Lagrange multiplier λ is related to the total energy constraint. With the help of Eq. (2) and Eq. (6), the difference of the ionic signals can be written as

$$P^{[1]}(t_0,T)-P^{[2]}(t_0,T)=\int_{-T}^{T}dt'\int_{-T}^{T}dt''K(t',t'')\mathcal{E}(t')\mathcal{E}^*(t'') \tag{9}$$

with the kernel

$$K(t',t'')=\alpha_1(t')\alpha_1^*(t'')-\alpha_2(t')\alpha_2^*(t''). \tag{10}$$

Here,

$$\alpha_i(t)\equiv\sum_n\langle f=0|n\rangle\langle n|0\rangle\exp[iE_n^{[i]}(t-t_0)]. \tag{11}$$

The variation of J with respect to the field $\mathcal{E}(t)$ is given by

$$\delta J=\int_{-T}^{T}dt'\int_{-T}^{T}dt''K(t',t'')[\mathcal{E}(t')\delta\mathcal{E}^*(t'')+\mathcal{E}^*(t'')\delta\mathcal{E}(t')]-\lambda\int_{-T}^{T}dt'[\mathcal{E}(t')\delta\mathcal{E}^*(t')+\mathcal{E}(t')^*\delta\mathcal{E}(t')]. \tag{12}$$

It follows immediately that the functional J takes a stationary value if $\mathcal{E}(t)$ obeys the integral equation

$$\int_{-T}^{T}dt'K(t',t)\mathcal{E}(t')=\lambda\mathcal{E}(t). \tag{13}$$

We can further identify the physical meaning of the Lagrange multiplier λ. By comparing Eq. (13) with Eq. (9) we find that

$$\lambda=\frac{P^{[1]}(t_0,T)-P^{[2]}(t_0,T)}{I} \tag{14}$$

is the yield of separation per pulse energy, and the global optimal field is associated with the largest value of $|\lambda|$ [32]. For a given value of t_0, the optimal fields are provided by two solutions of the integral equation (13),

$$\mathcal{E}^{(\pm)}(t)=\mathcal{N}^{(\pm)}[\alpha_1^*(t;t_0)-f^{(\pm)}(t_0,T)\alpha_2^*(t;t_0)] \tag{15}$$

with

$$f^{(\pm)}(t_0,T)=\frac{\lambda^{(\pm)}-C_{11}}{C_{12}}. \tag{16}$$

The normalization constant $\mathcal{N}^{(\pm)}$ is determined by the energy constraint condition Eq. (8). The two solutions for $\lambda^{(\pm)}$ are

$$\lambda^{\pm}(t_0,T)=\frac{1}{2}[C_{11}-C_{22}\mp\sqrt{(C_{11}+C_{22})^2-4|C_{12}|^2}]. \tag{17}$$

The coefficients C_{ij} are given by

$$C_{ii}=\int_{-T}^{T}dt|\alpha_i(t)|^2=2\sum_{n\neq m}p_{nm}\exp[-i(E_n^{[i]}-E_m^{[i]})t_0]\times\frac{\sin[(E_n^{[i]}-E_m^{[i]})T]}{E_n^{[i]}-E_m^{[i]}}+2T\sum_n p_{nn},$$

$$C_{12}=\int_{-T}^{T}dt\alpha_1^*(t)\alpha_2(t)=2\sum_{n,m}p_{nm}\exp[-i(E_n^{[1]}-E_m^{[2]})t_0]\times\frac{\sin[(E_n^{[1]}-E_m^{[2]})T]}{E_n^{[1]}-E_m^{[2]}}, \tag{18}$$

where $p_{nm}\equiv\langle f=0|n\rangle\langle m|f=0\rangle\langle n|0\rangle\langle 0|m\rangle$. Equation (17) enables us to calculate the yield of the control, $\lambda^{(\pm)}$, as a function of t_0. At the final stage of optimization, the maximal (minimal) values of this function should be found, providing us with the globally optimal fields.

III. RESULTS

We illustrate the use of the above method by simulating wave-packet isotope separation of an isotopic mixture of $^{79}Br_2$ and $^{81}Br_2$ molecules. The computations are done using Morse potentials with parameters taken from [33] and [34]. The involved potentials and Franck-Condon factors are shown in Fig. 2.

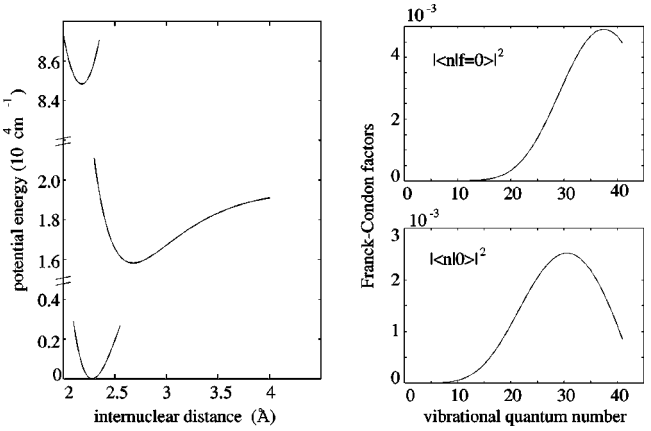

FIG. 2. Morse potential curves of Br_2 (a), and distribution of Franck-Condon factors for the transitions $|0\rangle|g\rangle \rightarrow |n\rangle|e\rangle$ (b) and $|n\rangle|e\rangle \rightarrow |0\rangle|i\rangle$ (c).

A. Isotope enrichment due to spatial separation of wave packets

The maximal yield of separation per unit pulse energy is given by the global maximum (minimum) of the function $\lambda^{(\pm)}(t_0,T)$. Figure 3(a) shows $\lambda^{(\pm)}(t_0,T)$ as a function of the ionization time t_0 for the interaction window of $2T = 0.27$ ps. This corresponds approximately to one-quarter of the vibrational period for levels lying in the Franck-Condon absorption maximum ($n \approx 31$). A maximum of $\lambda^{(-)}(t_0,T)$ corresponds to the enhanced ionization of $^{79}Br_2$ while a minimum of $\lambda^{(+)}(t_0,T)$ indicates enhanced ionization of $^{81}Br_2$. Global extrema of $\lambda^{(\pm)}(t_0,T)$ emerge around $t_0 \approx 9$ ps and $t_0 \approx 18$ ps.

The details of the process that leads to the maximal separation at $t_0 = 18.43$ ps, when $\lambda^{(+)}(t_0,T)$ has a minimum, are shown in Figs. 4(a)–4(c). The excitation field [Fig. 4(a)] consists of a single laser pulse that is short compared to $2T$. Immediately after the excitation, the wave packets in both isotopes are identical and cannot be distinguished by the ionization pulse. The excited population $n^{[i]}(t) = \Sigma_n |c_n^{[i]}(t)|^2$ [see Fig. 4(c)] is indeed virtually the same for both isotopes. As the excitation is not isotopically selective, the separation

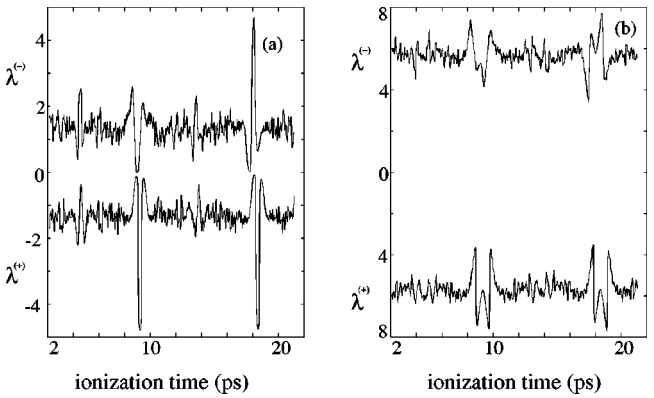

FIG. 3. The yield of separation per unit pulse energy, $\lambda^{(\pm)}(t_0,T)$, is plotted in arbitrary units as a function of the ionization time t_0. In (a), the interaction window is $2T = 0.27$ ps, in (b) it is $2T = 1.37$ ps.

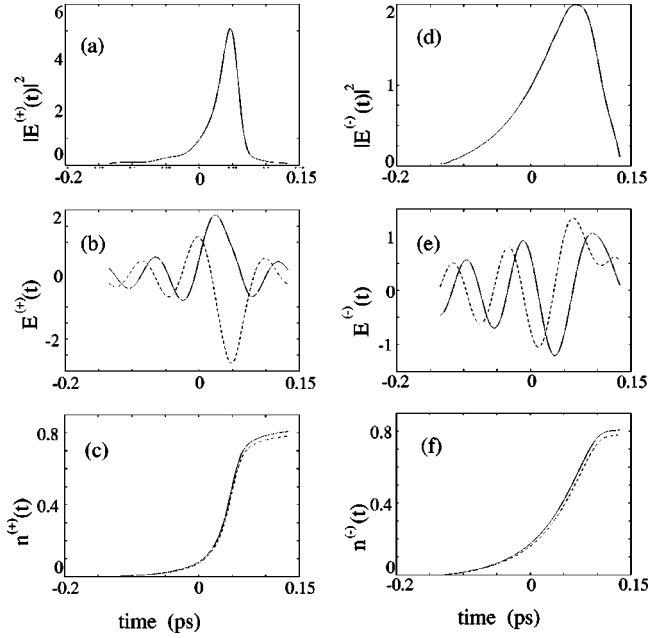

FIG. 4. Isotope enrichment through spatial separation: (a)–(c) show the details of the excitation process for $2T = 0.27$ ps and $t_0 = 18.45$ ps. The intensity of the optimal field, $|\mathcal{E}(t)|^2$, is plotted in (a). The real (solid line) and imaginary (dashed line) parts of $\mathcal{E}(t)$ are displayed in (b). (The carrier frequency, corresponding to the transition from $|0\rangle|g\rangle \rightarrow |31\rangle|e\rangle$, is extracted.) The population in the excited molecular potential, $n^{[i]}(t)$, during the excitation is shown in (c). Here, the solid and dashed lines correspond to the isotopes $^{79}Br_2$ and $^{81}Br_2$, respectively. The same quantities are displayed in (d)–(f) for $t_0 = 18.1$ ps. The optimal field and the population are plotted in arbitrary units.

can occur only due to differences in the free evolution of the wave packets of different isotopes. It can be seen in Fig. 5(a) that at $t = t_0$ the wave packets are, in fact, spatially separated. The wave packet of the $^{81}Br_2$ isotope (dashed line) is localized near the left turning point of the potential. Hence, the ionization probability for $^{81}Br_2$ is large, while the wave packet of $^{79}Br_2$, situated in the right half of the potential, is almost not affected by the ionization process. The preferential ionization of the latter isotope, $^{79}Br_2$, can be, of course, achieved by a similar separation process. The optimal ionization time for it ($t_0 = 18.1$ ps) is determined by the global maximum of $\lambda^{(-)}(t_0,T)$ [Fig. 3(a)], and the details of the process are displayed in Figs. 4(d)–4(f). The corresponding spatial probability density distribution at ionization time $t = t_0$ is plotted in Fig. 5(b).

This separation scheme, which came out automatically from our optimization procedure, is, actually, very close to that described in [14]. Indeed, the optimal ionization times found in Fig. 3(a) correspond to half and full revivals of a wave packet whose central energy lies in the region of the Franck-Condon absorption maximum. In addition, molecules of one of the isotopes are compressed, while molecules of the second one are stretched at the moment of ionization [see Fig. 5(a) and Fig. 5(b)]. These are exactly the conditions described in [14]. For the given interaction window $2T = 0.27$ ps, our procedure finds the best way to realize the

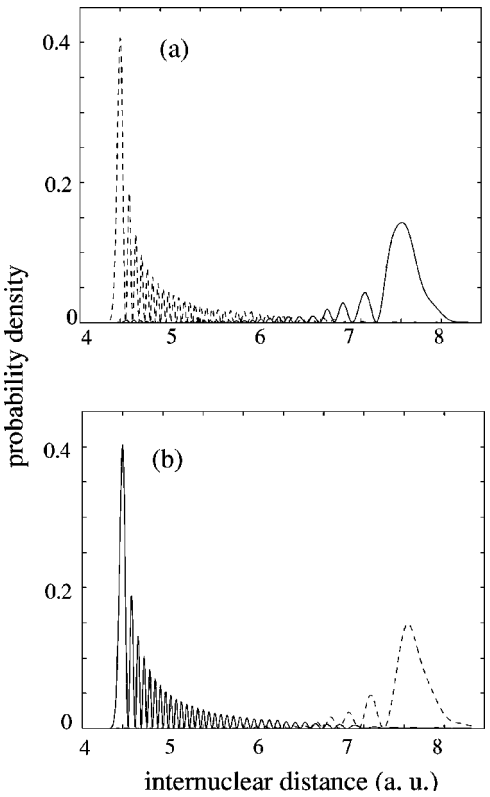

FIG. 5. Probability density at ionization time: In (a), the probability density (arbitrary units) is plotted at $t_0=18.45$ ps, in (b) at $t_0=18.1$ ps. In both cases, the interaction window was $2T=0.27$ ps. The solid line denotes the isotope $^{79}Br_2$ and the dashed line denotes $^{81}Br_2$.

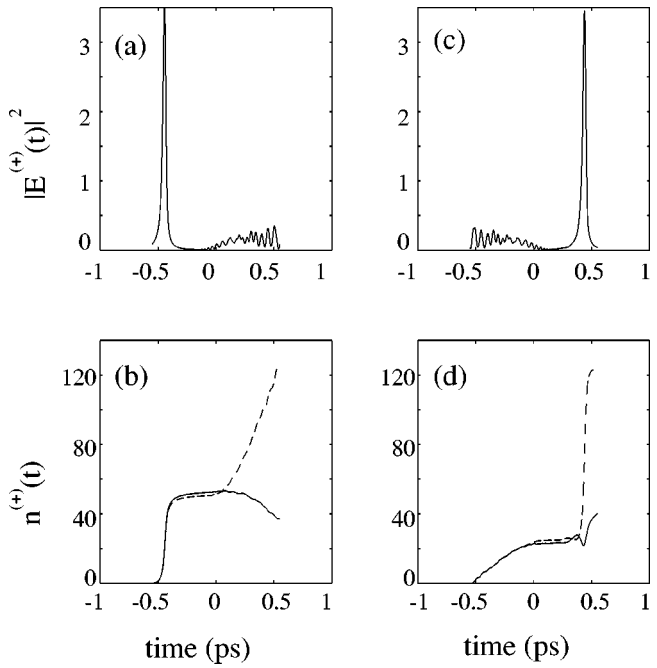

FIG. 6. Isotope separation through ''pump and dump'' mechanism: The upper graphs show the intensity of the optimal field, $|\mathcal{E}(t)|^2$ (arbitrary units), for $t_0=8.75$ ps (a) and for $t_0=9.63$ ps (b). The interaction window $2T=1.37$ ps is used in both cases. Graphs (c) and (d) show the corresponding population $n^{[i]}(t)$ (arbitrary units). As before, the solid and dashed lines correspond to the isotopes $^{79}Br_2$ and $^{81}Br_2$, respectively.

above scenario. Note that pulses *optimal* for preferential ionization of different isotopes are not the same [compare Fig. 4(a) and Fig.4(d)]. These optimal pulses are much shorter than single vibrational periods, and excite a large number of nonequidistant vibrational levels. As a result, the revival events are even shorter than a vibrational period, and different pulse shapes are needed to localize the specific isotopic wave packet at the left edge of the potential.

B. Isotope separation through ''pump and dump'' mechanism

It came out of our study that spatial separation between wave packets belonging to different isotopes is not the only mechanism to achieve isotope separation. Another way of reaching isotopically selective ionization is to suppress the population of one of the isotopes already during the excitation pulse. This mechanism appears in our optimization scheme when the interaction window $2T$ is longer than one vibrational period.

In Fig. 3(b), the interaction window is chosen to be $2T=1.37$ ps, which is approximately one-and-a-quarter of a vibrational period for levels lying in the Franck-Condon absorption maximum. When compared with Fig. 3(a), some differences attract attention. First, neither $\lambda^{(+)}(t_0,T)$ nor $\lambda^{(-)}(t_0,T)$ ever reach zero. This indicates that a part of the separation is already reached during the excitation process, and it may be further improved at the ionization stage, depending on the ionization time t_0. As in Fig. 3(a), the extreme values for $\lambda^{(\pm)}(t_0,T)$ can be found for $t_0\approx 9$ ps and $t_0\approx 18$ ps. In contrast to Fig. 3(a), we have now two almost equal minima (maxima) for each case.

We choose the optimal solutions for $t_0=8.75$ ps and for $t_0=9.61$ ps to demonstrate how the separation process works in this case. Figures 6(a) and 6(c) show the calculated optimal fields, which look like a pair of two separate laser pulses. Figures 6(b) and 6(d) display the change of the population in the intermediate potential during the interaction with the laser field. As before, the first laser pulse excites virtually identical wave packets of both isotopes, but, under the action of the second pulse of the pair, the population of one of the isotopes decreases while the population of the other increases. This means that there is a considerable enrichment of excited molecules by one of the isotopes immediately after the excitation stage. The two optimal fields displayed in Figs. 6(a) and 6(c) have a similar structure, except for the fact that the two pulses appear in reverse order.

The basis of this enrichment mechanism is the quantum interference phenomenon. Since the chosen interaction time is longer than one vibrational period, the wave packets return to the interaction region (left turning point) when the laser field is still on. This causes constructive or destructive interference in the excitation process. Constructive interference occurs if the wave packets excited by the first and the second pulse, respectively, have the same overall quantum-mechanical phase while destructive interference happens when they are out of phase. Our optimization procedure de-

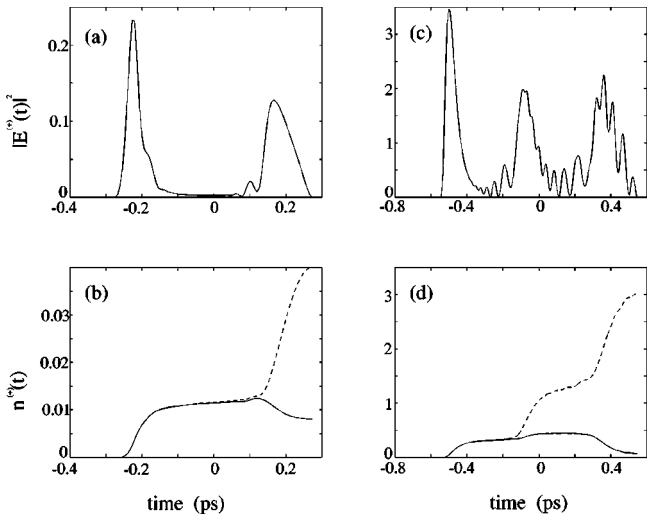

FIG. 7. ''Pump and dump'' mechanism for a laser pulse with restricted bandwidth: (a) shows the intensity of the optimal field (arbitrary units) for the interaction time $2T=0.5$ ps. (b) displays the excited population (arbitrary units) during the excitation for both isotopes. In (c) and (d), the interaction time is $2T=1.1$ ps. Again, the solid and dashed lines correspond to the isotopes $^{79}Br_2$ and $^{81}Br_2$, respectively.

fined a pulse sequence providing constructive interference for one of the isotopes and, at the same time, destructive interference for the other isotopic component. The second stage of the separation process is the ionization of the enriched isotope. As described in Sec. III A, the most efficient ionization can be achieved if the ionizing pulse is applied during a revival event of the wave packet [see Fig. 3(b)].

Let us indicate the different origin of isotope separation in the ''pump and dump'' mechanism and in the mechanism of spatial separation of wave packets described in the preceding section. Spatial separation depends on the difference in the vibrational periods, that is, on the difference in the *spacing* between subsequent energy levels in different isotopes. The

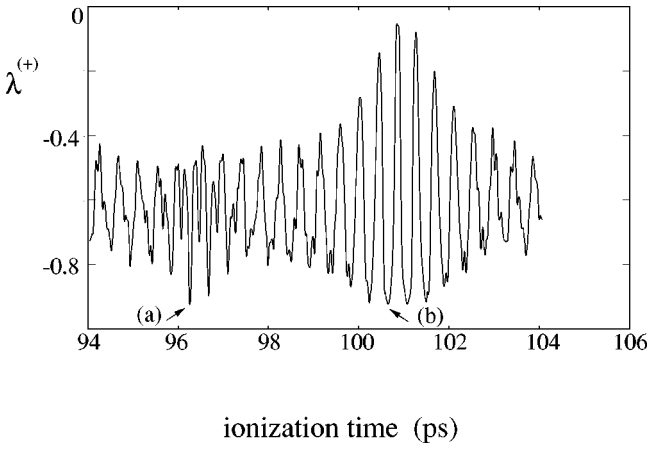

FIG. 8. The yield of separation per unit pulse energy, $\lambda^{(\pm)}(t_0,T)$ (arbitrary units), as a function of the ionization time t_0. The bandwidth of the laser pulse is restricted, so that only levels with $n\leqslant 25$ can be populated. The interaction window is $2T=0.26$ ps.

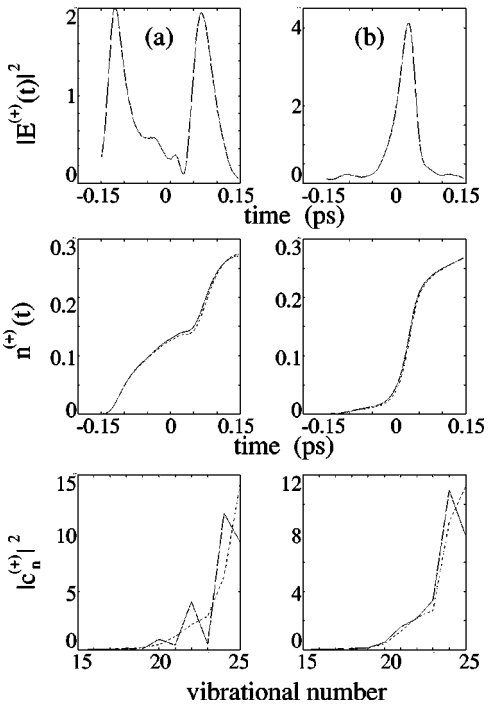

FIG. 9. Isotope separation and fractional revivals: Pulse intensity, $|\mathcal{E}(t)|^2$, population $n^{[i]}(t)$ during the excitation, and energy distribution $|c_n^{[i]}|^2$ after the excitation, all displayed in arbitrary units, for the interaction times $t_0=96.26$ ps (a) and $t_0=101.09$ ps (b). The interaction window is $2T=0.26$ ps.

''pump and dump'' mechanism is based on interference of transition amplitudes between different electronic states and, therefore, depends on the absolute position of the vibrational energy levels. For highly excited vibrational states, there is a considerable shift between energy levels in different isotopes despite the close values of their vibrational frequencies. Therefore, isotope enrichment in the ''pump and dump'' scheme occurs already after one vibrational period while separation of the wave packets takes much longer.

As in the previous case, our optimization procedure provides us with the best realization of the above described ''pump and dump'' scenario. It can be seen in Fig. 6(a) that the two pulses have very different shapes. The first, short, pulse excites wave packets containing a large number of nonequidistant vibrational levels. After a vibrational period, these wave packets are already dispersed, and a pulse of a different shape is needed to achieve the required interference.

In order to investigate the ''pump and dump'' scheme for ''longer living'' wave packets, we reduce the wave-packet spreading by restricting the spectral width of the excitation field. In Fig. 7, the maximal excitation energy is chosen to be approximately $E^{[i]}_{n=25}$. In Fig. 7(a) and Fig. 7(b), the interaction window is $2T=0.55$ ps. This is again one-and-a-quarter of a vibrational period for levels lying in the absorption maximum of the (now restricted) excitation spectrum. Here, the two pulses of the ''pump and dump'' scheme can be seen more clearly.

The isotopic enrichment of excited molecules can be even increased by further enlarging the interaction time. As an

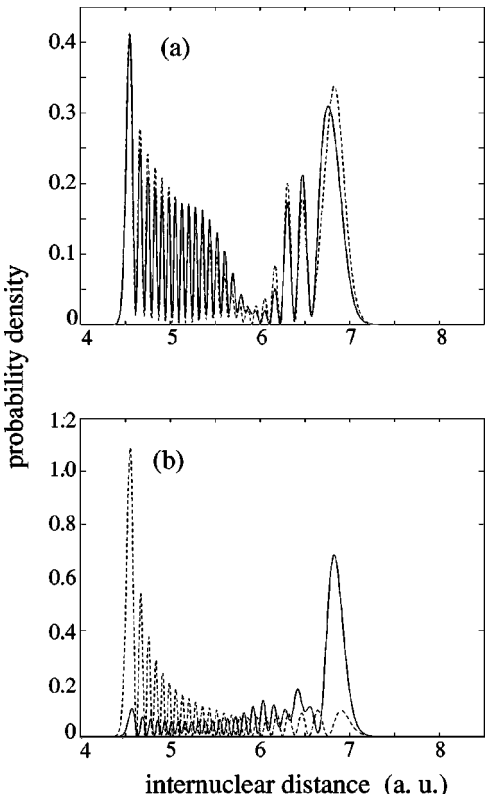

FIG. 10. Probability density of wave packets excited by the pulse sequence shown in Fig. 9(a). In (a), the probability density is plotted for $t=0.29$ ps (half a vibrational period after the excitation) and in (b) for $t=t_0=96.27$ ps. The solid and dashed lines correspond to the isotopes $^{79}Br_2$ and $^{81}Br_2$, respectively.

example, the optimal excitation process for an interaction window of $2T=1.1$ ps is shown in Fig. 7(c) and Fig. 7(d). Here, the interaction window is open for two-and-a-half vibrational periods, and hence a sequence of three pulses causes constructive or destructive interaction between three wave packets.

C. Isotope separation and fractional revivals

Until now we have focused the discussion on the cases in which the optimal ionization time t_0 corresponded to half or full revival times of the excited wave packet. However, the optimal separation may also occur at ionization times that correspond to fractional revivals of the wave packet, which means, at times, when the wave packet is split into two (or more) partial wave packets. To illustrate this point, we refer to Fig. 8, which displays $\lambda^{(+)}(t_0,T)$ as a function of the ionization time t_0. In this case, we restricted the spectrum of the laser field so that only levels with $n\leqslant 25$ can be excited. The interaction window is chosen to be $2T=0.26$ ps, which corresponds to 0.6 of a vibrational period for levels lying in the absorption maximum region. Note that due to the restriction of the excitation bandwidth, the spreading of the wave packets is reduced, and the revival event lasts for several vibrational periods. Pronounced minima of $\lambda^{(+)}(t_0,T)$ are found not only in the vicinity of a far-lying (half) revival event (b), but also at times corresponding to a neighboring

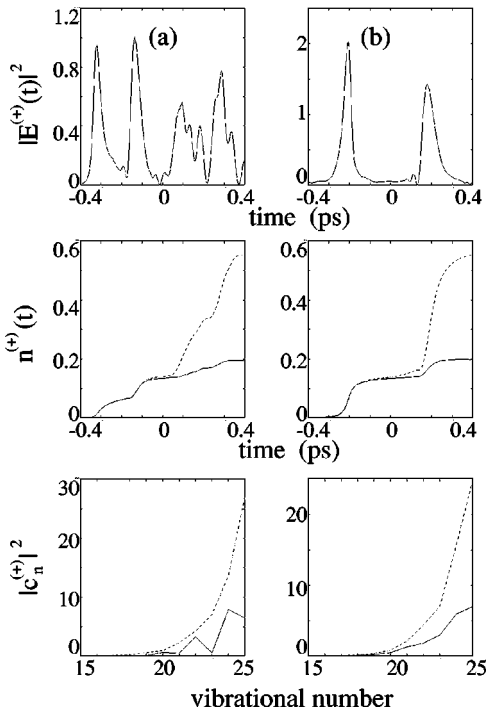

FIG. 11. Intensity of the excitation field, $|\mathcal{E}(t)|^2$, population $n^{[i]}(t)$ during the excitation, and energy distribution $|c_n^{[i]}|^2$ after the excitation, for $t_0=96.05$ ps (a) and $t_0=100.86$ ps (b). The interaction window is $2T=0.7$ ps.

quarter revival of the wave packet (a). The details of the respective excitation processes are shown in Fig. 9(a) and Fig. 9(b). If the ionization time corresponds to a half-revival event (b), the optimal field contains a single short pulse, and the separation occurs due to the spatial separation of the wave packets, as it was described in Sec. III A. If the ionization time is close to one-quarter revival time (a), the optimal field consists of a sequence of two pulses. The excitation process is, nevertheless, not isotopically selective: the total population $n^{[i]}(t)$ after the excitation is the same for both isotopes. While the energy distribution $|c_n|^2$ is smooth for the one-pulse excitation, it is oscillating in the two-pulse case: every second energy level is less populated.

The two pulses, shifted approximately by one-half of a vibrational period, excite two separate wave packets in each of the isotopes [see Fig. 10(a)]. The spectral composition of these wave packets is such that they form a *single* localized wave packet after a quarter of the revival time [see Fig. 10(b)]. Immediately after the excitation, the wave packets of different isotopes overlap, but due to the differences in their free evolution, the final wave packets are spatially separated at the ionization time $t=t_0$. It is interesting to note that here our optimization procedure ''rediscovered'' the idea of using fractional revivals for merging several wave packets in a single one at the target time. This approach was realized experimentally in Rydberg atoms [35] and discussed as a general control technique in Ref. [36].

A similar separation mechanism can be observed for a longer interaction window. Figures 11(a) and 11(b) show the optimal excitation procedure for the interaction window of $2T=0.7$ ps, which corresponds to 1.6 vibrational periods for

levels lying in the absorption maximum. Again, we find optimal solutions near the half-revival event [Fig. 11(b)] as well as near one-quarter revival [Fig. 11(a)]. Figure 11(b) displays the optimal field and the time evolution of the total excited population. The latter is characteristic for the ''pump and dump'' mechanism we described in Sec. III B. In Fig. 11(a), the optimal field contains a sequence of four pulses instead of two. They are needed to provide interference control over a two-component wave packet.

IV. SUMMARY

In this paper, we have demonstrated how optimal control theory can be used to explore the concept of wave-packet laser isotope separation. We developed a linear optimal control procedure for selective two-photon ionization of isotopic mixtures of diatomic molecules. Then we applied it to Br_2 molecules that were already used in first wave-packet isotope separation experiments [14]. Two main separation scenarios were identified. The first is based on the spatial separation of vibrational wave packets due to the isotopic mass difference. The second (''pump and dump'' mechanism) makes use of quantum interference produced by several laser pulses acting on the same electronic transition. Wave-packet isotope separation is closely related to the phenomenon of revivals (full and fractional), which provides the means for suppression of unwanted dispersion of quantum wave packets. We discovered various modifications of the above two basic scenarios, which depend on the specific kind of fractional revival involved in separation. In this work, we dealt only with weak laser fields. A further extension would be a nonlinear optimal control method for strong fields, which would allow us to separate a considerable amount of isotopic species.

ACKNOWLEDGMENTS

We would like to acknowledge support from the Minerva Foundation, the U.S.–Israel Binational Science Foundation, the Israel Ministry of Absorption (Center for Absorption of Scientists), and the Fritz Haber Center for Physical Chemistry.

[1] A.H. Zewail, *Femtochemistry* (World Scientific, Singapore, 1994), Vols.1 and 2.
[2] J. Manz and W. Ludger, *Femtosecond Chemistry* (VCH, Weinheim, 1995).
[3] A.M. Weiner and J.P. Heritage, Rev. Phys. Appl. **22**, 1619 (1987).
[4] T.C. Weinacht, J. Ahn, and P.H. Bucksbaum, Phys. Rev. Lett. **80**, 5508 (1998); Nature (London) **397**, 233 (1999).
[5] P. Brumer and M. Shapiro, Faraday Discuss. Chem. Soc. **82**, 177 (1986); M. Shapiro and P. Brumer, J. Chem. Phys. **84**, 4103 (1986); M. Shapiro and P. Brumer, Int. Rev. Phys. Chem. **13**, 187 (1994).
[6] D.J. Tannor and S.A. Rice, J. Chem. Phys. **83**, 5013 (1985); D.J. Tannor and S.A. Rice, Adv. Chem. Phys. **70**, 441 (1988); R. Kosloff, S.A. Rice, P. Gaspard, S. Tersigni, and D.J. Tannor, Chem. Phys. **139**, 201 (1989); J. Somloi, V.A. Kazakov, and D.J. Tannor, *ibid.* **172**, 85 (1993).
[7] A. Peirce, M. Dahleh, and H. Rabitz, Phys. Rev. A **37**, 4950 (1988); R.S. Judson and H. Rabitz, Phys. Rev. Lett. **68**, 1500 (1992); W.S. Warren, H. Rabitz, and M. Dahleh, Science **259**, 1581 (1993); H. Rabitz, R. de Vivie-Riedle, M. Motzkus, K. Kompa, *ibid.* **288**, 824 (2000).
[8] R.J. Gordon and S.A. Rice, Annu. Rev. Phys. Chem. **48**, 601 (1997).
[9] A. Assion, T. Baumert, M. Bergt, T. Brixner, B. Kiefer, V. Seyfied, M. Strehle, and G. Gerber, Science **282**, 919 (1998); T. Brixner, M. Strehle, and G. Gerber, Appl. Phys. B: Lasers Opt. **68**, 281 (1999); M. Bergt, T. Brixner, B. Kiefer, M. Strehle, and G. Gerber, J. Phys. Chem. A **103**, 10 381 (1999); O. Rubner, T. Baumert, M. Bergt, B. Kiefer, G. Gerber, and V. Engel, Chem. Phys. Lett. **316**, 585 (2000).
[10] I.Sh. Averbukh and M. Shapiro, Phys. Rev. A **47**, 5086 (1993); D.G. Abrashkevich, I.Sh. Averbukh, and M. Shapiro, J. Chem. Phys. **101**, 9295 (1994).
[11] B.M. Goodson, D. Goswami, H. Rabitz, and W.S. Warren, J. Chem. Phys. **112**, 5081 (2000).
[12] J. Heufelder, H. Ruppe, S. Rutz, E. Schreiber, and L. Woste, Chem. Phys. Lett. **269**, 1 (1997).
[13] S. Rutz and E. Schreiber, Eur. Phys. J. D **4**, 151 (1998).
[14] I.Sh. Averbukh, M.J.J. Vrakking, D.M. Villeneuve, and A. Stolow, Phys. Rev. Lett. **77**, 3518 (1996).
[15] For a review, see P.T. Greenland, Contemp. Phys. **30**, 405 (1990).
[16] W. H. King, *Isotope Shifts in Atomic Spectra* (Plenum, New York, 1984).
[17] J.H. Eberly, N.B. Narozhny, and J.J. Sanchez-Mondragon, Phys. Rev. Lett. **44**, 1323 (1980).
[18] J. Parker and C.R. Stroud, Jr., Phys. Rev. Lett. **56**, 716 (1986).
[19] I.Sh. Averbukh and N.F. Perelman, Phys. Lett. A **139**, 449 (1989); Zh. Éksp. Teor. Fiz. **96**, 818 (1989) [Sov. Phys. JETP **69**, 464 (1989)]; Usp. Fiz. Nouk **162**, 41 (1991) [Sov. Phys. Usp. **34**, 572 (1991)].
[20] M. Nauenberg, Phys. Rev. A **40**, 1133 (1989); J. Phys. B **23**, L385 (1990).
[21] C. Leichtle, I.Sh. Averbukh, and W.P. Schleich, Phys. Rev. Lett. **77**, 3999 (1996); Phys. Rev. A **54**, 5299 (1996).
[22] R. Bluhm, V.A. Kostelecký, and J.A. Porter, Am. J. Phys. **64**, 944 (1996).
[23] J.A. Yeazell, M. Mallalieu, and C.R. Stroud, Jr., Phys. Rev. Lett. **64**, 2007 (1990); J.A. Yeazell and C.R. Stroud, Jr., Phys. Rev. A **43**, 5153 (1991).
[24] D.R. Meacher, P.E. Meyler, I.G. Hughes, and P. Ewart, J. Phys. B **24**, L63 (1991).
[25] J. Wals, H.H. Fielding, J.F. Christian, L.C. Snoek, W.J. van der Zande, and H.B. van Linden van den Heuvell, Phys. Rev. Lett. **72**, 3783 (1994); J. Wals, H.H. Fielding, and H.B. van Linden van den Heuvell, Phys. Scr., **T58**, 62 (1995).
[26] L. Marmet, H. Held, G. Raithel, J.A. Yeazell, and H. Walther,

Phys. Rev. Lett. **72**, 3779 (1994); G. Raithel, H. Held, L. Marmet, and H. Walther, J. Phys. B **27**, 2849 (1994).

[27] T. Baumert, V. Engel, C.R. Röttgermann, W.T. Strunz, and G. Gerber, Chem. Phys. Lett. **191**, 639 (1992); T. Baumert and G. Gerber, Isr. J. Chem. **34**, 103 (1994).

[28] I. Fischer, D.M. Villeneuve, M.J.J. Vrakking, and A. Stolow, J. Chem. Phys. **102**, 5566 (1995); M.J.J. Vrakking, D.M. Villeneuve, and A. Stolow, Phys. Rev. A **54**, R37 (1996).

[29] Ch. Meier and V. Engel, in *Femtosecond Chemistry*, edited by J. Manz and W. Ludger (VCH, Weinheim, 1995), Vol. 1.

[30] W.A. Chupka, in *Ion-Molecule Reactions*, edited by J.L. Franklin (Butterworth, London, 1972), Vol. 1.

[31] V. Engel, Chem. Phys. Lett. **178**, 130 (1991).

[32] Z. Shen, Y. Yan, J. Cheng, F. Shuang, Y. Zhao, and G. He, J. Chem. Phys. **110**, 7192 (1999); J. Cheng, Z. Shen, and Y. Yan, *ibid.* **109**, 1654 (1998).

[33] K. P. Huber and G. Herzberg, *Molecular Spectra and Molecular Structure* (Van Nostrand, New York, 1979), Vol. 4.

[34] T. Harris, J.H.D. Eland, and R.P. Tuckett, J. Mol. Spectrosc. **98**, 269 (1983).

[35] M.W. Noel and C.R. Stroud, Jr., Phys. Rev. Lett. **75**, 1252 (1995); **77**, 1913 (1996).

[36] X. Chen and J.A. Yeazell, Phys. Rev. A **59**, 3782 (1999).